

Delay Equalization by Tapered Cutoff Waveguides

CHARLES C. H. TANG

Summary—When a wave packet propagates in a guided mode subject to cutoff at a definite frequency, dispersion is always present. To restore the shapes of the wave packets at the receiving end, a proper delay equalization must be applied.

Waves propagating in a waveguide tapered to cutoff dimensions are reflected mostly in a region where the dimensions are at cutoff. Accordingly waves of higher frequencies will penetrate deeper into the tapered guide and thereby introduce more delay than those of lower frequencies. A profile of a tapered waveguide is obtained for the case of linear delay on the hypothetical assumption that a wave is totally reflected only at the plane of cutoff dimensions. The problem of finding a proper profile is similar in nature to the inverse scattering problem in quantum mechanics.

The complex input reflection coefficient introduced by a tapered cutoff waveguide is invariably unity in its magnitude for all frequencies below cutoff and has different phases for different frequencies. Presently available theory for computing the complex reflection coefficient is valid only when its magnitude is smaller than unity. A theoretical method to calculate with accuracy the phase of such unity reflection coefficient is presented.

The linking section between the standard waveguide and the tapered cutoff waveguide is designed on the basis of a high-pass filter that introduces no appreciable perturbation to the prescribed delay characteristic.

The excellent agreement between the theoretical results and measured data suggests that microwave delay equalizers can be designed "on paper" with "measurement" accuracy without even going to the laboratory. Accordingly the claim can be made that any reasonable amount of delay of simple shape within certain bandwidth limits can be equalized by the present approach.

INTRODUCTION

WHEN A WAVE PACKET propagates in a guided mode subject to cutoff at a definite frequency, dispersion is always present. For instance, in a long distance transmission system using the low-loss TE_{01} mode in a 2-inch circular waveguide, the cutoff frequency is at 7.203 kMc. Assuming the wave packet has a carrier frequency at 40.25 kMc and a bandwidth of 500 Mc, the delay due to dispersion within the band can be shown to decrease almost linearly with frequency, and its total differential "linear" delay is about 45 μ sec after traveling 20 miles. To restore the shape of the wave packet at the receiving end, an inverse delay shape must be applied. This restoring process is usually called delay equalization or compensation.

The subject of delay equalization based on the principle of cutoff reflection in a tapered waveguide was first proposed by J. R. Pierce in 1951 and later studied both

Manuscript received May 4, 1964; revised August 6, 1964.

The author is with Bell Telephone Laboratories, Inc., Murray Hill, N. J.

theoretically and experimentally by others.¹ The basic principle of delay equalization by cutoff reflection in a tapered waveguide depends on the fact that waves propagating in a tapered cutoff waveguide are reflected mostly in a region where the guide is at cutoff. Accordingly waves of higher frequencies penetrate deeper into the tapered section and thereby introduce more delay than those of lower frequencies. By properly shaping the tapered section its delay characteristic may be made to approximate any reasonable prescribed requirement.

This paper deals with two closely related problems—that of finding the profile of a tapered waveguide which yields a prescribed delay characteristic and that of calculating the delay characteristic of a nonuniform waveguide of an arbitrary mechanical profile. The available theory² for computing the complex input reflection coefficient ρ can be conveniently used with accuracy only when ρ is much smaller than unity. Accurate results for cases of ρ close to unity involve many complicated numerical integrations. Since the complex input reflection coefficient of a tapered cutoff waveguide is always unity (lossless case), the available theory cannot be vigorously used. A new method of accurately securing the phases of complex input reflection coefficients of unity and therefore delay is presented.

Another major problem is the design of a linking section between the standard waveguide and the tapered cutoff waveguide (equalizer proper). Since the largest dimension of the tapered section is the cutoff dimension of the lowest frequency of the band of interest, the smallest dimension of the linking section must have this cutoff dimension. The linking section with this cutoff dimension at one end must be of such a design that it does not perturb appreciably the delay characteristic of the tapered equalizer proper. A design procedure for such a linking section is described. The theoretical results thus obtained are in excellent agreement with the experimental data.

FORMULATIONS

When a wave of frequency f enters a tapered cutoff waveguide, it is clear that most of the wave will be reflected at the plane having cutoff dimensions at the frequency f , whereas some will be reflected along the

¹ W. J. Albersheim, R. E. Fisher, G. Szentirmai, and K. W. Woo, private communications.

² C. C. H. Tang, "Nonuniform waveguide high-pass filters with extremely steep cutoff," IEEE TRANS. ON MICROWAVE THEORY AND TECHNIQUES, vol. MTT-12, pp. 300-309; May, 1964.

path before that plane and some will penetrate beyond that plane before being reflected. To find the actual round-trip phase change of such propagation in a tapered waveguide is rather difficult. As a start, the problem shall be simplified by assuming that the wave is totally reflected only at the plane of the cutoff dimensions. In this hypothetical case the wave, propagating in the x direction, will undergo a round-trip phase change in radians by an amount,

$$\phi = 2 \int \beta(f, x) dx = \frac{4\pi f \sqrt{\epsilon_r \mu_r}}{C} \int_0^{x_f} \sqrt{1 - \left(\frac{f_e}{f}\right)^2} dx, \quad (1)$$

with

$$\beta(f, x_f) = 0, \quad (2)$$

where C is the velocity of light, x_f is the distance (from the entrance of the taper) at which the cutoff dimensions of frequency f occur, and f_e is the cutoff frequency and is a function of distance x as shown below. For circular waveguide

$$f_e = \frac{C k_{mn}}{2\pi \sqrt{\epsilon_r \mu_r} a(x)}, \quad (3)$$

where k_{mn} is the n th root of Bessel function J_m , and $a(x)$ is the radius of the circular waveguide at the distance x with $a(0) = a_0$. For rectangular waveguide

$$f_e = \frac{mC}{2\sqrt{\epsilon_r \mu_r} a(x)}, \quad (4)$$

where m is the mode number of the rectangular guide H_{m0} mode, and $a(x)$ is the width at the distance x with $a(0) = a_0$.

The corresponding delay is by definition

$$\begin{aligned} \tau = \frac{d\phi}{d\omega} &= \frac{2\sqrt{\epsilon_r \mu_r f}}{C} \int_0^{x_f} \frac{dx}{\sqrt{f^2 - f_e^2}} \\ &= \frac{2\sqrt{\epsilon_r \mu_r f}}{C} \int_{a_0}^{a_f} \frac{da}{\sqrt{f^2 - f_e^2}}. \end{aligned} \quad (5)$$

Substituting (3) or (4) into (5), we have

$$\tau = \frac{2\sqrt{\epsilon_r \mu_r}}{C} \int_{a_0}^{a_f=p} \frac{a \frac{da}{da}}{\sqrt{a^2 - p^2}} da, \quad a_0 \geq a \geq p, \quad (6)$$

where

$$p(f) = \frac{C k_{mn}}{2\pi f \sqrt{\epsilon_r \mu_r}} = \frac{k_{mn}}{2\pi} \lambda_0 \quad \text{for circular guide,} \quad (7a)$$

and

$$p(f) = \frac{mC}{2f \sqrt{\epsilon_r \mu_r}} = \frac{m}{2} \lambda_0 \quad \text{for rectangular guide.} \quad (7b)$$

If the delay characteristic is prescribed, the particular profile that yields the required delay characteristic can be obtained by inverting, if possible, the integral equation (6).

The inversion³ of (6) can be accomplished in the following manner. Multiplying both sides of (6) by $p/\sqrt{p^2 - \mu^2}$ and integrating with respect to p ,

$$\begin{aligned} \frac{C}{2\sqrt{\epsilon_r \mu_r}} \int_{a_0}^u \frac{\tau(p) p dp}{\sqrt{p^2 - u^2}} \\ = \int_{a_0}^u \frac{p dp}{\sqrt{p^2 - u^2}} \int_{a_0}^p \frac{\frac{dx}{da} da}{\sqrt{a^2 - p^2}}. \end{aligned} \quad (8)$$

Interchanging the order of integration and performing the necessary operations, we get the slope of the profile

$$\frac{dx}{da} = - \frac{C}{\sqrt{\epsilon_r \mu_r}} \frac{1}{\pi a} \frac{d}{da} \int_{a_0}^a \frac{\tau(p) p dp}{\sqrt{p^2 - a^2}}. \quad (9)$$

For linear delay, with the aid of (7),

$$\tau = \frac{\tau_m}{\Delta f} (f - f_l) = \frac{\tau_m f_l}{\Delta f} \left(\frac{f}{f_l} - 1 \right) = \frac{\tau_m f_l}{\Delta f} \left(\frac{a_0}{p} - 1 \right), \quad (10)$$

where τ_m is the maximum differential delay within the band, $\Delta f = f_h - f_l$, and f_h and f_l are respectively the highest and lowest frequency of the band. Substitution of (10) into (9) gives

$$\begin{aligned} \frac{dx}{da} &= \frac{C}{\sqrt{\epsilon_r \mu_r}} \frac{\tau_m f_l}{\pi a (\Delta f)} \frac{d}{da} \left[a_0 \cosh^{-1} \frac{a_0}{a} + \sqrt{p^2 - a^2} \right] \\ &= \frac{C}{\sqrt{\epsilon_r \mu_r}} \frac{\tau_m f_l}{\pi a (\Delta f)} \left[\frac{\sqrt{a_0^2 - a^2}}{a} \right]. \end{aligned} \quad (11)$$

Integration of (11) yields the sought-for profile

$$x = \frac{C \tau_m f_l}{\sqrt{\epsilon_r \mu_r} \pi (\Delta f)} \left[\frac{\sqrt{a_0^2 - a^2}}{a} - \cos^{-1} \frac{a}{a_0} \right]. \quad (12)$$

In passing, we note that this problem of finding a proper profile is similar in nature to the inverse scattering problem in quantum mechanics.

Having obtained the mechanical profile of (12) for the linear delay characteristic on the hypothetical assumption that a wave is totally reflected only at the plane of cutoff dimensions, one now attempts to find out theoretically what is the actual delay characteristic of such a profile, *i.e.*, how much it deviates from the linear one.

³ C. H. Page, "Physical Mathematics," D. Van Nostrand Company, Inc., Princeton, N. J., p. 174; 1955.

The complex input reflection coefficient² ρ of a non-uniform waveguide section of length l is

$$\rho(0) = \frac{\rho_0 e^{-j\theta} + \left[\int_0^l k e^{-2j\theta} dx + \int_0^l k e^{-2j\theta} \int_0^x k(x') e^{2j\theta(x')} \int_0^x k(x'') e^{-2j\theta(x'')} dx'' dx' dx + \dots \right]}{1 + \left[\int_0^l k e^{-j2\theta} \int_0^x k(x') e^{2j\theta(x')} dx' dx + \dots \right]} \quad (13)$$

where

$$k = \frac{1}{2} \frac{d}{dx} \log_b Z_c \quad (14)$$

$$\theta = \int_0^x \beta dx \quad (15)$$

and

ρ_0 is the reflection coefficient at the termination,
 Z_c is the nominal characteristic impedance,
 μ is the nominal phase constant.

Eq. (13) is valid when ρ is smaller than unity. Since the complex input reflection coefficient ρ of a tapered cutoff waveguide section is always unity in magnitude within our frequency band of interest, (13) is no longer suitable here. To find accurately the phase of a unity reflection coefficient and therefore the delay from a smoothly tapered cutoff waveguide of given profile, one resorts to the method of forming the tapered profile into steps of extremely thin depth as shown in Fig. 1. The formulation for obtaining an accurate complex input reflection coefficient of such a step configuration of very thin depth is presented below.

The matrix representation of the two-port configuration of Fig. 1 that relates the voltage (V_{n+1}) and current (I_{n+1}) at the input port to their corresponding quantities (V_0 and I_0) at the output port, has the following well-known form,

$$\begin{bmatrix} V_{n+1} \\ I_{n+1} \end{bmatrix} = \begin{bmatrix} A & B \\ C & D \end{bmatrix} \begin{bmatrix} V_0 \\ -I_0 \end{bmatrix}, \quad (16)$$

where, neglecting the small capacitive effects at the steps,

$$\begin{bmatrix} A & B \\ C & D \end{bmatrix} = \prod_{s=n+1}^1 \begin{bmatrix} a_s & b_s \\ c_s & d_s \end{bmatrix} \begin{bmatrix} 1 & 0 \\ 1/Z_L & 1 \end{bmatrix}, \quad (17)$$

where Z_L is the load impedance. Now with the aid of the transmission line equations in input-output form one easily identifies that in (17)

$$a_n = d_n = \cosh(j\beta_n l_n) = \cos \beta_n l_n, \quad (18)$$

and

$$b_n = Z_{cn}^2 c_n = Z_{cn} \sinh(j\beta_n l_n) = j Z_{cn} \sin \beta_n l_n, \quad (19)$$

where Z_{cn} and β_n are respectively the normalized nominal characteristic impedance and nominal phase con-

stant of the n th short straight section in Fig. 1. The input reflection coefficient ρ_b and the transmission coefficient t_b can be obtained from the scattering matrix \bar{S} :

$$\bar{S} = \begin{bmatrix} S_{bb} & S_{be} \\ S_{eb} & S_{ee} \end{bmatrix}, \quad (20)$$

and one has the reflection coefficient

$$\rho_b = S_{bb}, \quad (21)$$

and the transmission coefficient

$$t_b = S_{be}. \quad (22)$$

The phases of the unity input reflection coefficients of such a step configuration will depend on the number of steps we choose. A minimum number of steps is preferred for simpler computation and easier precision machining. On the other hand, the number of steps must be such that when it is increased, the phases of the unity input reflection coefficients remain substantially constant. When such a minimum number of steps is chosen, it can be assured that the computed phases obtained from such a step configuration are those of a corresponding smooth profile. The number of steps necessary for a given profile depends on the frequency of the carrier used, and usually is smaller for lower frequencies.

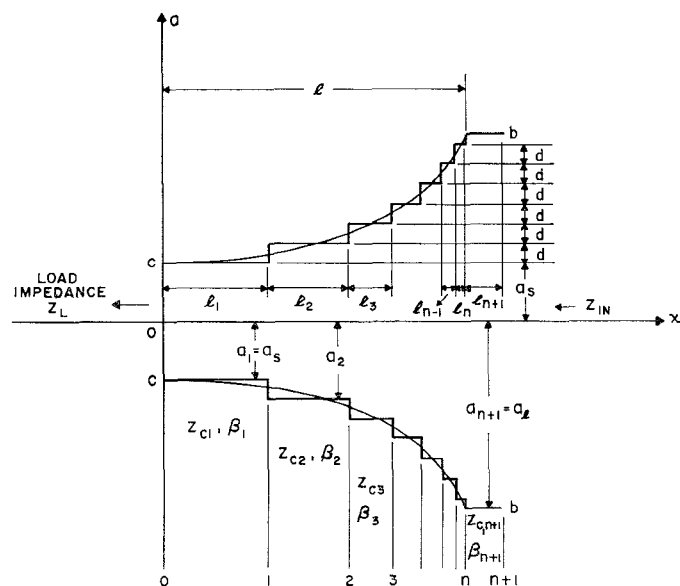


Fig. 1—Step configuration (equal step depth d).

DESIGNS

It is appropriate at this point to consider the problem of choosing the carrier frequency to be used from the viewpoint of design convenience since the bandwidth is conserved in that it is independent of the carrier chosen. From the standpoint of reducing the length of the tapered equalizer proper to a minimum, one should use the highest possible carrier frequency because of the fact that the length is approximately proportional to $(\Delta f/f)^{1/2}$. This can be shown from (12) with $a_0 - a = \Delta a \approx 1$, that

$$x \approx \frac{C\tau_m f}{3\pi\sqrt{\epsilon_r\mu_r}(\Delta f)} \left(\frac{\sqrt{a_0^2 - a^2}}{a} \right)^3 = \frac{2\sqrt{2}C\tau_m f}{3\pi\sqrt{\epsilon_r\mu_r}(\Delta f)} \left(\frac{\Delta a}{a} \right)^{3/2}$$

$$= \frac{2\sqrt{2}C\tau_m}{3\pi\sqrt{\epsilon_r\mu_r}} \left(\frac{\Delta f}{f} \right)^{1/2}. \quad (23)$$

On the other hand, from the standpoint of reducing the difficulties in precision machining the transverse dimensions of the tapered equalizer proper, one should use the lowest possible carrier frequency because of the fact that the maximum transverse dimensional change is proportional to $(\Delta f/f^2)$. A circular waveguide tapered equalizer shall be used since it is easier to machine with precision a tapered circular guide than a tapered rectangular guide. A comparison of the required lengths and transverse dimensions for three different waveguide sizes is made in Table I. It appears that the H_{11} mode at 11 kMc is a good compromise.

TABLE I

| Frequency | Length | Change in diameter |
|-----------|--|---|
| 4 kMc | $\left(\frac{11}{4}\right)^{1/2} \cdot 34$ inch | $\left(\frac{11}{4}\right)^2 \cdot 28.62$ mils |
| 11 kMc | 34 inch | 28.62 mils |
| 40 kMc | $\left(\frac{11}{40}\right)^{1/2} \cdot 34$ inch | $\left(\frac{11}{40}\right)^2 \cdot 28.62$ mils |

Theoretically it might be advantageous to use H_{mn} mode other than H_{11} in order to obtain a larger change in diameter for easier fabrication; however, the choice of H_{11} mode is dictated by the availability of a low reflection (-45 db from 10.75 to 11.25 kMc) transducer from circular to rectangular guide. Rectangular waveguides are required for the experimental standing wave measurements since precision standing wave detectors are commercially available only in rectangular waveguides.

The above discussion gives us enough information to obtain the sought for tapered profile from (12) with the following data.

$\tau_m = 47 \mu\text{sec}$ (added 2 μsec to be explained later)

$f_l = 10.75 \text{ kMc}$

$\Delta f = 11.25 - 10.75 = 0.5 \text{ kMc}$

$a_0 = 0.321955 \text{ inch.}$

$$a = \frac{Ck_{11}}{2\pi f \sqrt{\epsilon_r\mu_r}}$$

$k_{11} = 1.84118$

$\epsilon_r = 1$

$\mu_r = 1$

a varies from 0.321955 inch to 0.307646 inch.

The total length of the tapered section turns out to be 35.1996 inches. The actual profile of the taper is shown in Fig. 2 and its hypothetical linear delay characteristic and computed theoretical delay characteristic obtained by (21) are shown in Fig. 3. The computed delay is obtained by numerical differentiation of phases with respect to frequencies. It is clear from Fig. 3 that the computed delay does have an average delay characteristic which is nearly identical with the hypothetical linear delay except at the two ends. Excluding the ends the computed characteristic is found to have a maximum ripple of about $\pm 1 \mu\text{sec}$. The large deviations at the low-frequency end can be explained by the fact that there is a discontinuity in the slope dx/da at the entrance end ($a = a_0$) of the tapered equalizer since in computing the delay the tapered equalizer is assumed to be connected to a straight guide of radius a_0 . The effect of this discontinuity in slope in computing the delay is evident from (5) or (6). Accordingly one is justified in ignoring for the moment the large deviation of delay at the low-frequency end. It will be corrected later when an appropriate linking section is introduced between the tapered equalizer proper and a straight waveguide of standard radius for 11 kMc. The large deviations at the high-frequency end can be explained by the fact that the tapered equalizer proper is terminated by a matched load in computing the delay. In doing so some of the waves at the high-frequency end are absorbed entirely by the matched termination after penetrating beyond the cutoff dimensions and thereby are reflected with less reflection and delay. This can be corrected, to be shown later, by extending the small radius end of the equalizer a few more inches in a straight section. The computed delay characteristic of Fig. 3 is obtained by machining the equalizer in steps of 0.0004 inch in depth. Any further decrease in step depth does not change the delay shape.

To measure experimentally the delay characteristic of the tapered equalizer a linking section must be provided between the standard waveguide for 11 kMc and the tapered equalizer. There are apparently a few different lines of philosophy in pursuing the design of the linking section. The simplest way is to extend the design of the

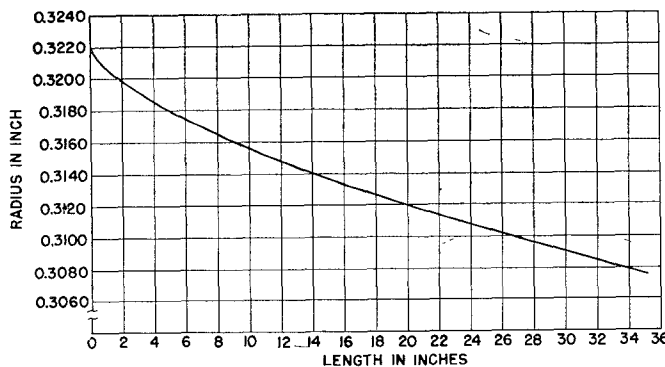


Fig. 2—The mechanical profile of the tapered equalizer.

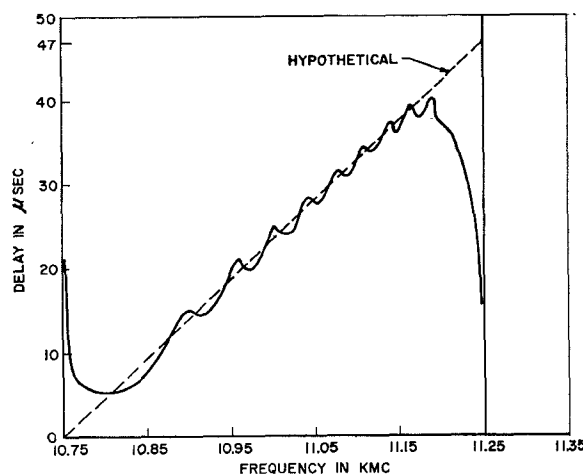


Fig. 3—Comparison of hypothetical linear delay and computed theoretical delay.

tapered equalizer until it can be connected directly to the standard waveguide of radius 0.375 inch for 11 kMc operation. Setting the large end radius of the tapered equalizer equal to 0.375 inches makes its lowest cutoff frequency at 9.23 kMc and thus will extend the bandwidth to about 2 kMc for linear delay. For such wide bandwidth the length of the equalizer will be almost twice as long as that for 500 Mc bandwidth according to (23). This scheme, therefore, does not seem to be attractive. A possible modification of the above scheme is to shift the carrier frequency closer to the cutoff frequency, 9.23 kMc, of the standard waveguide in order to reduce the unused bandwidth. For instance, the carrier frequency can be moved to 10 kMc, and the unused bandwidth of the equalizer can be reduced to about 500 Mc. In this case some of the components required in experimental measurements, *e.g.*, the transducer for circular H_{11} mode to rectangular H_{01} mode, will have to be redesigned for very low reflections around 10 kMc. Accordingly this scheme is not too attractive either.

A third scheme is that of designing a near cutoff high-pass filter that will introduce minimum perturbation on the characteristic of the equalizer proper. From the experience obtained in designing nonuniform symmetrical

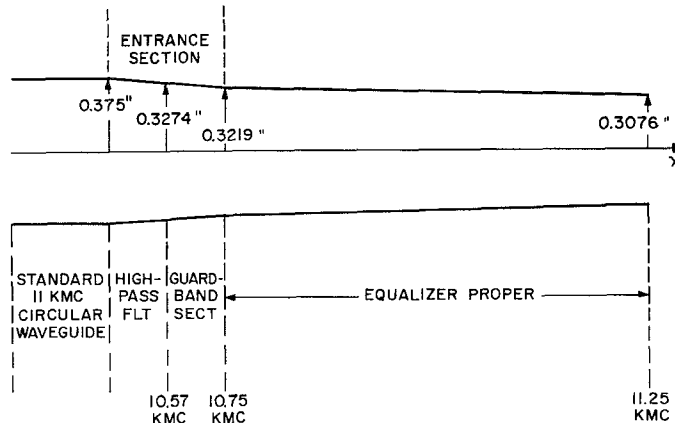


Fig. 4—Diagrammatic arrangement for delay equalization.

high-pass filters² at 40 to 80 kMc, it is known that reflections can be reduced to about -50 db within 0.33 per cent of the cutoff frequency, *e.g.*, within 0.18 kMc at 50 kMc cutoff. We propose to design as a first trial a nonsymmetrical high-pass filter which reduces reflections to about -30 db within 1.6 per cent of the cutoff frequency near 11 kMc, *i.e.*, within 0.18 kMc. This means the nonsymmetrical high-pass filter should cut off at 10.57 kMc so that at 10.75 kMc the reflection is -30 db. The introduction of such a high-pass filter indicates that we need another linking section to connect the high-pass filter end of 0.3274 inch radius (10.57 kMc) to the equalizer end of 0.3219 inch radius (10.75 kMc). In order to avoid confusion, this linking or transition section between the high-pass filter and the equalizer proper shall be designated as the guard-band section and the cascaded section of high-pass filter and guard-band section as the entrance section. This is diagrammatically shown in Fig. 4. The purpose of using the cascaded section instead of one single high-pass filter as the entrance section is an attempt to reduce reflections near the cutoff end since tapered high-pass filters of smaller differential change in dimensions at the two ends will introduce lower reflections near the cutoff frequency and yield steeper reflection characteristics.

From the design procedure to be described later, one is able to obtain the characteristics of the entrance section as shown in Fig. 5. It is seen that the entrance section introduces within the 10.81 to 11.25 kMc band less than -30 db reflection and about 2 μ sec total differential transmission delay. To compensate for this 2 μ sec extra "linear" delay due to the entrance section, an equalizer proper must be designed that yields 47 μ sec linear delay instead of 45 μ sec as shown in Fig. 3.

Having obtained the necessary information on the entrance section which can link the standard waveguide at one end and the equalizer proper at the other end, one is now in a position to see what is the effect of the entrance section on the delay characteristic of the equalizer proper. The over-all delay characteristic to the input plane of the entrance section when followed by the

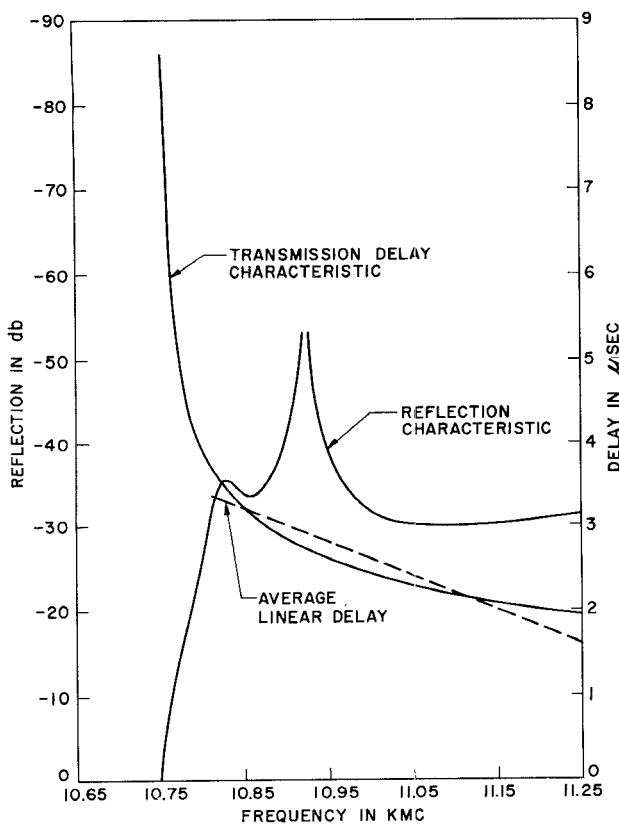


Fig. 5—Combined characteristics of the high-pass filter and guard-band section.

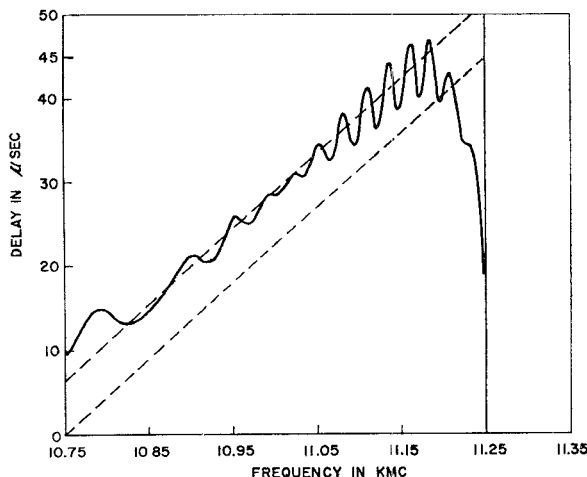


Fig. 6—Computed delay characteristic of the configuration shown in Fig. 4.

equalizer proper, is shown in Fig. 6. Comparison of Fig. 6 with Fig. 3 shows that the total differential average linear delay is 45 μ sec within the band as anticipated and the delay ripples are slightly decreased for the low-frequency portion and increased for the high-frequency portion. The results indicate that there is room for improvement on the design of the entrance section so that the ripples in the over-all delay characteristic can be reduced, especially at the high-frequency portion. However, before modifying the design, let us examine some experimental data.

EXPERIMENTAL MEASUREMENTS

The phase and therefore delay was measured by the conventional standing wave detector method. Measurements were made in standard rectangular waveguide by using a very low reflection (-45 db around 11 kMc) $H_{11}^{\circ}-H_{11}^{\square}$ transducer. Fig. 7 shows the measured overall delay characteristic and attenuation characteristic of the combination of the entrance section and the equalizer proper. The total length of the combination is 45.1996 inches (entrance section 8 inches, equalizer proper 35.1996 inches and 2 inches straight extension at the end of the equalizer proper for wave penetration at the high frequency end of the band).

The theoretical delay curve of Fig. 6 modified at the high-frequency end by adding the 2-inch straight extension is fitted to into the measured delay points of Fig. 7 and the excellent agreement between the measured and theoretical results is evident.

The measured attenuation curve is obtained because of the near cutoff and cutoff attenuation in the tapered guide. It is seen from Fig. 7 that the actual input reflection coefficient is steadily decreasing from unity with increasing frequency, and at 11.25 kMc the voltage reflection coefficient is about 0.7, corresponding to 3 db attenuation. The theoretical near cutoff attenuation per unit length for circular waveguides is given by the approximate equation,

$$\alpha_{mn} = \frac{R_s}{a} \sqrt{\frac{\epsilon_1}{g_1}} \frac{1}{\sqrt{1 - \xi^2}} \cdot \left[\xi^2 + \frac{m^2}{k_{mn}^2 - m^2} \right] \text{ nepers/m,} \quad (24)$$

with

$$R_s = \sqrt{\frac{\pi f \mu_2}{\sigma_f}} \quad \text{and} \quad \xi = \left(\frac{f_c}{f} \right). \quad (25)$$

For our circular waveguide with dominant mode propagation, we have

$$m = 1, \quad n = 1,$$

and

$$k_{11} = 1.84.$$

The attenuation per second for the H_{11} mode then is

$$C_{H_{11}} = \frac{C}{a} \left(\frac{\epsilon_1 \mu_2 C k_{11}}{2 \mu_1 \sigma_2 \xi_a} \right)^{1/2} (\xi^2 + 0.42) \text{ nepers/sec.} \quad (26)$$

For air-filled copper waveguide of $a = 0.308$ inch, one has an attenuation of about 3.45×10^7 db per sec. For a total delay of 52 μ sec (45 μ sec plus 7 μ sec flat delay) at 11.25 kMc the total attenuation is about 1.8 db. Considering the approximate nature of (24) and the fact that it does not take into account the extra attenuation

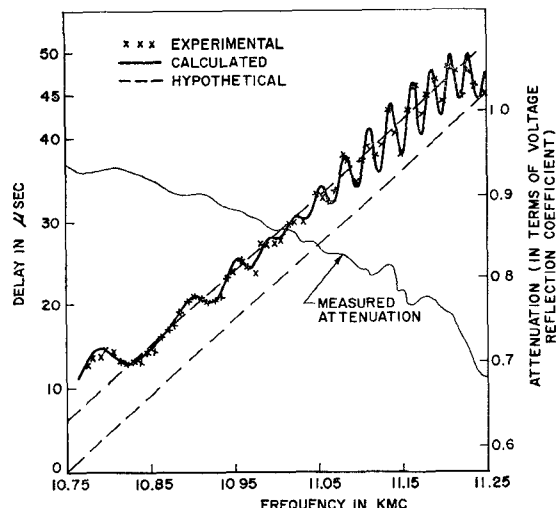


Fig. 7—Over-all delay and attenuation characteristics of configuration shown in Fig. 4 plus a 2-inch straight extension.

due to wave penetration beyond cutoff dimensions, one would say that a deviation around 1 db is rather reasonable.

IMPROVEMENTS

After verifying the excellent agreement between the measured and theoretical results, one is confident that the delay ripples at the high frequencies can be reduced if the design of the entrance section can be improved. Inspection of Fig. 5 for the entrance section indicates that its reflection characteristic at the high-frequency portion must be improved in order to reduce the relatively larger ripples at the high-frequency end of Figs. 6 or 7, even at the expense of introducing more reflections near the cutoff end.

With the aid of information presented elsewhere,² we choose for both the high-pass filter section and guard-band section the following profile:

$$a = \frac{\lambda_p}{\left[1 - \left(1 - \frac{\lambda_p^2}{a_s^2} \right) \left[\frac{1 - \left(\frac{\lambda_p}{a_s} \right)^2 \cos^2(\pi/2)(x/l)}{1 - \left(\frac{\lambda_p}{a_s} \right)^2} \right]^{1/2} \right]} \quad (27)$$

where a_s and a_l are, respectively, the dimensions of the small and large end of the filter, and $\lambda_p = (k_{mn}/2\pi) \lambda_{op}$ with k_{mn} as the n th root of Bessel function J_m and λ_{op} as the free space wavelength of the particular frequency chosen near cutoff. The profile of (27) corresponds to the characteristic impedance variation along the filter as follows:

$$Z_c = C e^{\epsilon \cos^2 \left(\frac{\pi x}{2l} \right)} \quad (28)$$

It is cut into steps as shown in Fig. 1 with step depth of 0.0002 inch. Its reflection characteristic and transmission delay characteristic are calculated by (20) and shown in Figs. 8 and 9 respectively. Comparison of Fig.

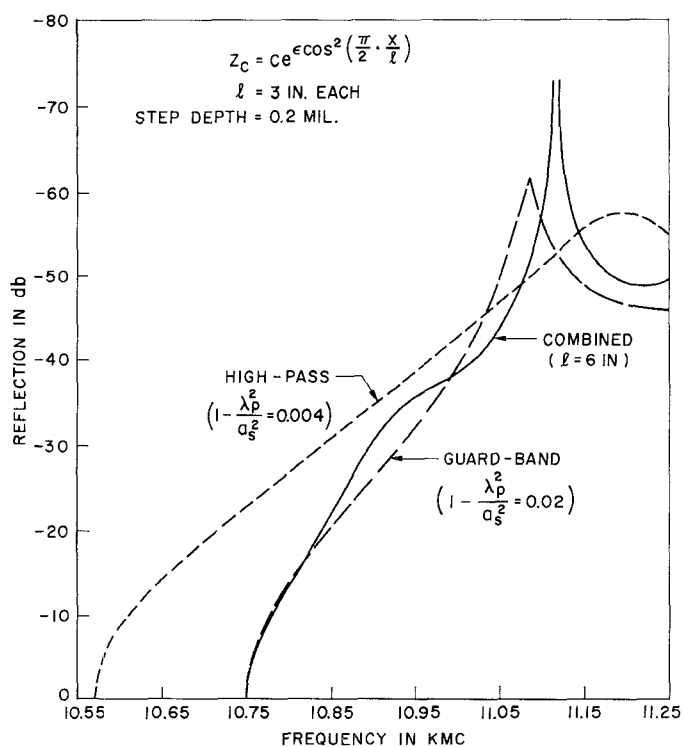


Fig. 8—Reflection characteristic of improved design for the entrance section.

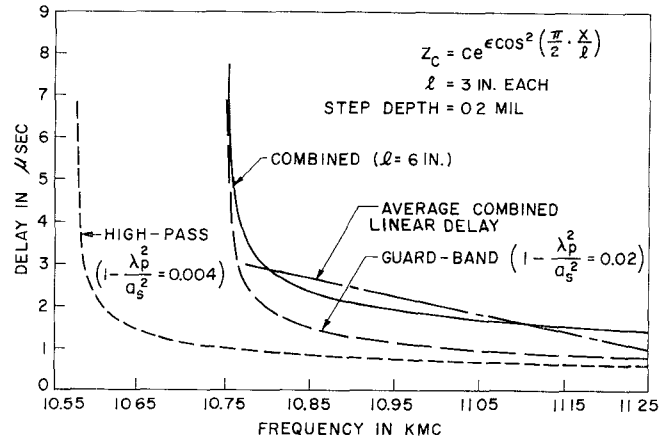


Fig. 9—Transmission delay characteristic of improved design for the entrance section.

8 with Fig. 5 shows that the reflections at the high-frequency portion have been reduced at least 20 db whereas those at the low-frequency end increased about 10 db. On the other hand the transmission delay is improved noticeably at the low-frequency end, since the 2 μ sec average delay of Fig. 9 can now cover 475 Mc instead of the 440 Mc shown in Fig. 5. This improvement of delay should be noticeable also in the improved over-all delay characteristic of Fig. 10 obtained by connecting the improved entrance section, equalizer proper, and a 3-inch-long straight extension in cascade. The expected improvements both at the low-frequency end and high-frequency end are verified in Fig. 10 when compared with Fig. 7. It is seen from Fig. 10 that the average devi-

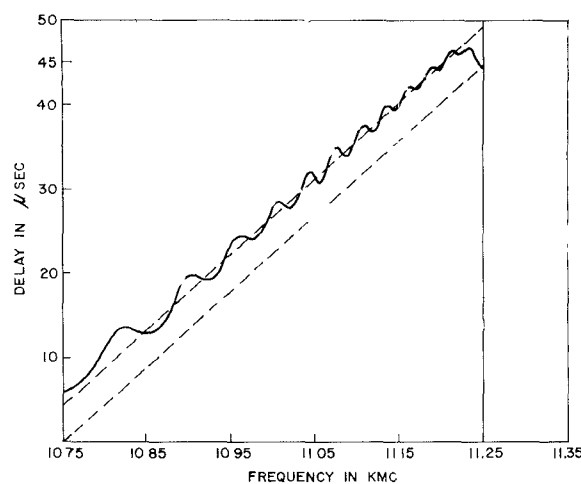


Fig. 10—Calculated over-all delay characteristic for improved design.

ation from linear delay is less than 1 μ sec for the entire frequency band of 500 Mc. Note the improved design also reduces the total length of the entrance section from 8 to 6 inches. It is important to note in passing that the increase of reflection of about 10 db at the low-frequency end of the reflection characteristic of the improved entrance section does not impair the over-all delay characteristic. This can be explained by the fact that for low frequencies of the band the equalizer proper alone presents nearly total reflections almost immediately and thereby introduces relatively small delays. Accordingly for the entrance section the improvement in transmission delays at low frequencies of the band is more important than that in reflection.

Comparison of the improved over-all delay characteristic of Fig. 10 with the corresponding delay characteristic (Fig. 3 to be modified at the high-frequency end) for the equalizer proper alone shows that the two characteristics have almost similar shape for the entire band except near the cutoff end. From this observation one is able to conclude that the improved entrance section virtually introduces no appreciable effect except the 2 μ linear delay which can be incorporated into the equalizer proper. On the assumption that an entrance

section that introduces no appreciable perturbations can be designed, it is clear that any further improvement in reducing the small ripples in the over-all delay characteristic must be made in the design of the equalizer proper. One of the simple and logical ways in attempting to accomplish that further improvement is to find a smooth equalizer profile that will yield the prescribed linear delay plus the inverse delay ripples of Fig. 3 between 10.8 and 11.25 kMc. However, a better profile than the one now used has not as yet been found.

CONCLUSIONS

It has been successfully demonstrated both theoretically and experimentally that a linear delay of 45 μ sec for a bandwidth of 500 Mc can be equalized to within 1 μ sec by near-cutoff reflections from a tapered waveguide of specific profile when the entrance section preceding the tapered waveguide is properly designed. Accordingly the claim can be made that any reasonable amount of delay of certain simple shape within any practical bandwidth can be equalized. For the case of linear delay the physical length of the tapered equalizer proper is directly proportional to both the amount of delay prescribed and the square root of the ratio of the required bandwidth to the chosen carrier frequency.

The design of the entrance section is basically in the nature of a high-pass filter. It consists of two high-pass filters in cascade, each of which has a distinct cutoff frequency. It is pertinent at this point to mention that probably one single high-pass filter of comparable length to link the standard waveguide directly to the equalizer proper would be sufficient, since it is now recognized that very low reflections near cutoff are not as important as those at the high-frequency end.

The agreement between the measured results and theoretical computations is astonishingly excellent.

ACKNOWLEDGMENT

The author wishes to thank N. Shellenberger for her consistent and patient interest and assistance in carrying out the computations, and W. D. Baker for the measurements.